

# Predicting Pedestrian Crossing Intention with Feature Fusion and Spatio-Temporal Attention

Dongfang Yang\*, Haolin Zhang\*, Ekim Yurtsever, Keith Redmill, *Senior Member, IEEE*, and Ümit Özgüner, *Life Fellow, IEEE*

**Abstract**—Predicting vulnerable road user behavior is an essential prerequisite for deploying Automated Driving Systems (ADS) in the real-world. Pedestrian crossing intention should be recognized in real-time, especially for urban driving. Recent works have shown the potential of using vision-based deep neural network models for this task. However, these models are not robust and certain issues still need to be resolved. First, the global spatio-temporal context that accounts for the interaction between the target pedestrian and the scene has not been properly utilized. Second, the optimum strategy for fusing different sensor data has not been thoroughly investigated. This work addresses the above limitations by introducing a novel neural network architecture to fuse inherently different spatio-temporal features for pedestrian crossing intention prediction. We fuse different phenomena such as sequences of RGB imagery, semantic segmentation masks, and ego-vehicle speed in an optimum way using attention mechanisms and a stack of recurrent neural networks. The optimum architecture was obtained through exhaustive ablation and comparison studies. Extensive comparative experiments on the JAAD pedestrian action prediction benchmark demonstrate the effectiveness of the proposed method, where state-of-the-art performance was achieved. Our code is open-source and publicly available: [https://github.com/OSU-Haolin/Pedestrian\\_Crossing\\_Intention\\_Prediction](https://github.com/OSU-Haolin/Pedestrian_Crossing_Intention_Prediction).

## I. INTRODUCTION

Predicting surrounding road user behavior is crucial for driving. This is especially prevalent during vehicle-pedestrian interactions. In urban areas, vehicles equipped with automated driving systems (ADS) and advanced driver-assistance systems (ADAS) frequently interact with crossing pedestrians, where intention prediction plays a vital role in decision-making. Nowadays, visual sensors such as front-facing cameras are becoming the standard configuration of intelligent vehicles. Therefore, vision-based prediction of pedestrian intention is promising and has a huge prospect of mass deployment.

Vision-based pedestrian crossing intention prediction has been explored for several years. Early works [1] usually utilized a single frame as input to a convolutional neural network (CNN) based prediction system. This approach ignores the temporal aspect of videos, which plays a critical role in intention prediction. Later on, with the maturity of recurrent neural networks (RNNs), pedestrian crossing intention was predicted by considering both the spatial and

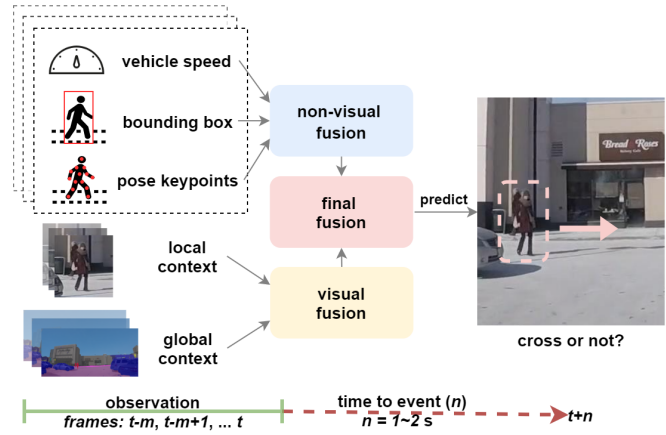


Fig. 1. Predicting pedestrian crossing intention is a multi-modal spatio-temporal problem. Our method fuses inherently different spatio-temporal phenomena with CNN-based visual encoders, RNN stacks, and attention mechanisms to achieve state-of-the-art performance.

temporal information [2], [3], [4]. This led to different ways of fusing different features, e.g., the detected pedestrian bounding boxes, poses, appearance, and even the ego-vehicle information [5], [6], [7], [8], [9]. The most recent benchmark of pedestrian intention prediction was released by [10], in which the PCPA model achieved the state-of-the-art in the most popular dataset JAAD [1]. However, PCPA lacks the consideration of global contexts such as road and other road users, which we believe is nonnegligible in pedestrian crossing intention prediction. Furthermore, the existing fusion strategies may not be optimal.

In this work, we focus on improving the performance of vision-based prediction of pedestrian crossing intention, i.e., whether a pedestrian detected by a front-facing camera will cross the road or not in a short time horizon (1-2s). Our work leverages the power of deep neural networks and fuses the features of both the local and the global context. Both non-visual and visual information are considered in our model, as illustrated in Figure 1. They are extracted from a sequence of video frames 1-2s before the crossing / not crossing (C/NC) event. Non-visual information includes the pedestrian's bounding box, pose keypoints, and ego-vehicle speed. Visual information contains local context and global context. Local context is the enlarged pedestrian appearance based on the bounding box position. Global context is the semantic segmentation of road, pedestrians (all pedestrians in the scene), and vehicles. They are used because they significantly affect the target pedestrian's crossing decision. We proposed a hybrid way of fusing the the non-visual and

\*Equal contribution.

Authors are with the Department of Electrical and Computer Engineering, The Ohio State University, Columbus, OH 43210, USA. Contact: [{yang.3455,zhang.10749,yurtsever.2,redmill.1,ozguner.1}@osu.edu](mailto:{yang.3455,zhang.10749,yurtsever.2,redmill.1,ozguner.1}@osu.edu)

visual features, which is justified by comparing different strategies of feature fusion.

Our main contributions are as follows:

- A novel vision-based pedestrian intention prediction framework for ADSs and ADASs. The proposed method employs a novel neural network architecture for utilizing different spatio-temporal features with a hybrid fusion strategy.
- Extensive ablation studies on different feature fusion strategies (early, later, hierarchical, or hybrid), input configurations (adding/removing input channels, using semantic segmentation masks as explicit global context), and visual encoder options (3D CNN or 2D convolution with RNN + attention) to identify the best model layout.
- Demonstrating the efficiency of the proposed method on the commonly used JAAD dataset [1], and achieving state-of-the-art performance on the most recent pedestrian action prediction benchmark [10].

## II. RELATED WORK

Vision-based pedestrian crossing prediction traces back to the works [11] that utilize the Caltech Pedestrian Detection Benchmark [12]. However, the Caltech dataset does not explicitly annotate the crossing behavior of the pedestrians. This gap was later filled by the introduction of JAAD dataset [1] that offers high-resolution videos and explicit crossing behavior annotations. With the release of JAAD dataset, a simple baseline was also created that uses a 2D convolutional neural network (CNN) to encode the features in a given previous frame and then uses a linear support vector machine (SVM) to predict the C/NC event.

**Spatio-temporal modeling.** Instead of using a single image, most recent works use image sequences as input to the prediction model due to the importance of temporal information in the prediction task. This leads to spatio-temporal modeling.

Spatio-temporal modeling can be achieved by first extracting visual (spatial) features per frame via 2D CNNs [13] or graph convolution networks (GCNs) [14], and then feeding these features into RNNs such as long-short term memory (LSTM) model [15] and gate recurrent unit (GRU) model [16]. For example, [2], [3], [4] use 2D convolution to extract the visual features from image sequence, and RNNs to encode the temporal information among these features. The encoded sequential visual features are fed into a fully-connected layer to obtain the final intention prediction.

Another way of extracting the sequential visual features is utilizing 3D CNN [17]. It directly captures the spatio-temporal features by replacing the 2D kernels of the convolution and the pooling layers in 2D CNN with 3D counterparts. For example, [18], [19] use 3D CNN based framework (3D DenseNet) to directly extract the sequential visual features from the pedestrian image sequence. The final prediction is achieved in a similar way of using a fully-connected layer.

The crossing intention prediction task can also be combined with scene prediction. A couple of works [20], [21] attempted to decompose the prediction task into two stages.

In the first stage, the model predicts a sequence of future scenes using an encoder/decoder network. Then, pedestrian actions are predicted based on the generated future scenes using a binary classifier.

**Feature fusion.** Instead of end-to-end modeling of visual features, information such as pedestrian's bounding box, body-pose keypoints, vehicle motion, and the explicit global scene context can also be modeled as separate channels as inputs to the prediction model. This requires a proper way of fusing the above information.

For example, [5], [22], [23], [24], [6] introduced human poses/skeletons in pedestrian crossing prediction tasks since human pose can be considered as a good indicator of human behaviors. By extracting the pose keypoints from cropped pedestrian images, crossing behavior classifiers are built based on the human pose feature vectors. Improvement in prediction accuracy shows the effectiveness of using pose features. However, these methods either only rely on human pose features without considering other important features or pay less attention to feature fusion.

Some other methods focused on novel fusion architecture. For instance, [7] proposed SF-GRU, a stacked RNN-based architecture, to hierarchically fuse five feature sources (pedestrian appearance, surrounding context, pose, bounding box, and ego-vehicle speed) for pedestrian crossing intention prediction. Nevertheless, this method does not take global context into account. [8] proposed a multi-modal based prediction system that integrates four feature sources (local scene, semantic map, pedestrian motion, and ego-motion). The global context (semantic map) is utilized, but it lacks other important features such as human pose. [9] proposed a multi-task based prediction framework to take advantages of feature sharing and multi-task learning. It fuses four feature sources (semantic map, pedestrians' trajectory, grid locations, and ego-motion). However, local context and human pose are not considered in the model.

Very recently, more datasets such as PIE [4] and PeP-Scenes [25] provide more annotations for fusing different features. A benchmark was also released with the PCPA model [10]. They create more room for researchers to explore the task of vision-based pedestrian crossing intention prediction.

## III. PROPOSED METHOD

### A. Problem formulation

The task of vision-based pedestrian crossing intention prediction is formulated as follows. Given a sequence of observed video frames from the vehicle's front view and the relevant information of ego-vehicle motion, the goal is to design a model that can estimate the probability of the target pedestrian  $i$ 's action  $A_i^{t+n} \in \{0, 1\}$  of crossing the road, where  $t$  is the specific time of the last observed frame and  $n$  is the number of frames from the last observed frame to the crossing / not crossing (C/NC) event.

In the proposed model, explicit features such as pedestrian's bounding box, pose keypoints, local context (cropped image around the pedestrian), and global context (semantic

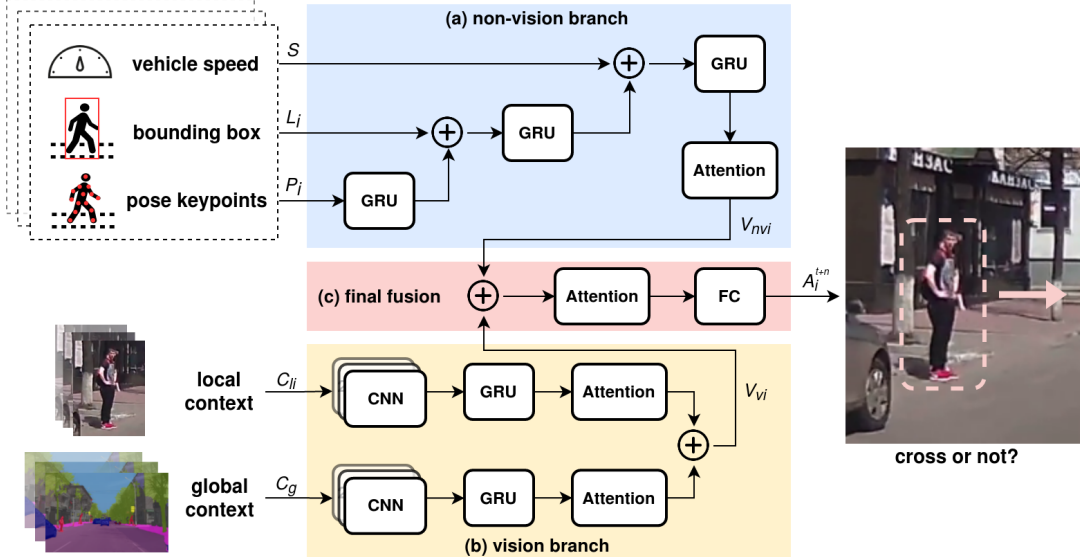


Fig. 2. **Overview of the proposed pedestrian crossing intention prediction model.** The yellow part denotes the fusion of visual features. 2D convolutional features of local context and global context are encoded by GRU and fed to the attention blocks respectively. Two outputs are concatenated as final visual features. The blue part denotes the fusion of local features (non-visual). These non-visual features are encoded by GRU and fused hierarchically, and then fed to an attention block to obtain the final non-visual features. The red part denotes the final fusion. Final visual features and final non-visual features are concatenated and fed to an attention block. A fully-connected (FC) layer is then applied to make the final prediction.

segmentation) are firstly extracted. They are used together with the vehicle’s speed as separate channels that serve as the input to the prediction model. Therefore, our model has the following input sources:

- The sequential local context around pedestrian  $i$ :  $C_{li} = \{c_{li}^{t-m}, c_{li}^{t-m+1}, \dots, c_{li}^t\}$ .
- The 2D location trajectory of pedestrian  $i$  denoted by bounding box coordinates (top-left points and bottom-right points):  $L_i = \{l_i^{t-m}, l_i^{t-m+1}, \dots, l_i^t\}$ .
- Pose keypoints of pedestrian  $i$ :  $P_i = \{p_i^{t-m}, p_i^{t-m+1}, \dots, p_i^t\}$ ;
- Speed of ego-vehicle:  $S = \{s^{t-m}, s^{t-m+1}, \dots, s^t\}$ ;
- The sequential global context denoted by the mask of semantic segmentation  $C_g = \{c_g^{t-m}, c_g^{t-m+1}, \dots, c_g^t\}$ .

Each source has a sequence of length  $m + 1$ . The input sources are also visualized in Figure 2.

## B. Input acquisition

**Local context and 2D location trajectory.** Local context  $C_{li}$  provides visual features of the target pedestrian. 2D location trajectory  $L_i$  gives the position change of the target pedestrian in the image. They can be extracted by a detection (e.g. YOLO [26]) and tracking (e.g. SORT [27]) system. In our work, we directly use the ground truth  $C_{li}$  and  $L_i$  from the dataset, because pedestrian detection and tracking are not the primary focus of this work. Specifically, the local context  $C_{li} = \{c_{li}^{t-m}, c_{li}^{t-m+1}, \dots, c_{li}^t\}$  consists of a sequence of RGB images of size [224, 224] pixels around the target pedestrian. The 2D location trajectory  $L_i = \{l_i^{t-m}, l_i^{t-m+1}, \dots, l_i^t\}$  consists of target pedestrian’s bounding box coordinates, i.e.,  $l_i^{t-m} = \{x_{it}^{t-m}, y_{it}^{t-m}, x_{ib}^{t-m}, y_{ib}^{t-m}\}$ , where  $x_{it}^{t-m}, y_{it}^{t-m}$  denotes the top-left point and  $x_{ib}^{t-m}, y_{ib}^{t-m}$  bottom-right point.

**Pedestrian pose keypoints.** Pedestrian pose keypoints represent the target pedestrian’s detailed motion, i.e., the posture at each frame while moving. They can be obtained by applying a pose estimation algorithm on the local context  $C_{li}$ . Since the applied JAAD dataset does not provide ground truth pose keypoints, we utilize pre-trained OpenPose model [28] to extract the pedestrian pose keypoints  $P_i = \{p_i^{t-m}, p_i^{t-m+1}, \dots, p_i^t\}$ , where  $p$  is a 36D vector of 2D coordinates that contain 18 pose joints, i.e.,  $p_i^{t-m} = \{x_{i1}^{t-m}, y_{i1}^{t-m}, x_{i2}^{t-m}, y_{i2}^{t-m}, \dots, x_{i18}^{t-m}, y_{i18}^{t-m}\}$ .

**Ego-vehicle speed.** Ego-vehicle speed  $S$  is a major factor that affects the pedestrian’s crossing decision. It can be directly read from the ego-vehicle’s system. Since the dataset contains the annotation of ego-vehicle’s speed, we directly use the ground truth labels for the vehicle speed  $S = \{s^{t-m}, s^{t-m+1}, \dots, s^t\}$ .

**Global context.** Global context  $C_g = \{c_g^{t-m}, c_g^{t-m+1}, \dots, c_g^t\}$  offers the visual features that account for multi-interactions between the road and road users, or among road users. In our work, we use pixel-level semantic masks to represent the global context. The semantic masks classify and localize different objects in the image by labeling all the pixels associated with the objects the a pixel value. Since the JAAD dataset does not have annotated ground truth of semantic masks, we use DeepLabV3 model [29] pretrained on Cityscapes Dataset [30] to extract the semantic masks and select important objects (e.g. road, street, pedestrians and vehicles) as the global context. For the model to learn the interactions between the target pedestrian  $i$  and these objects, the target pedestrian is masked by an unique label. The mask area uses the target pedestrian  $i$ ’s bounding box (obtained from  $L_i$ ). The semantic segmentation of all input

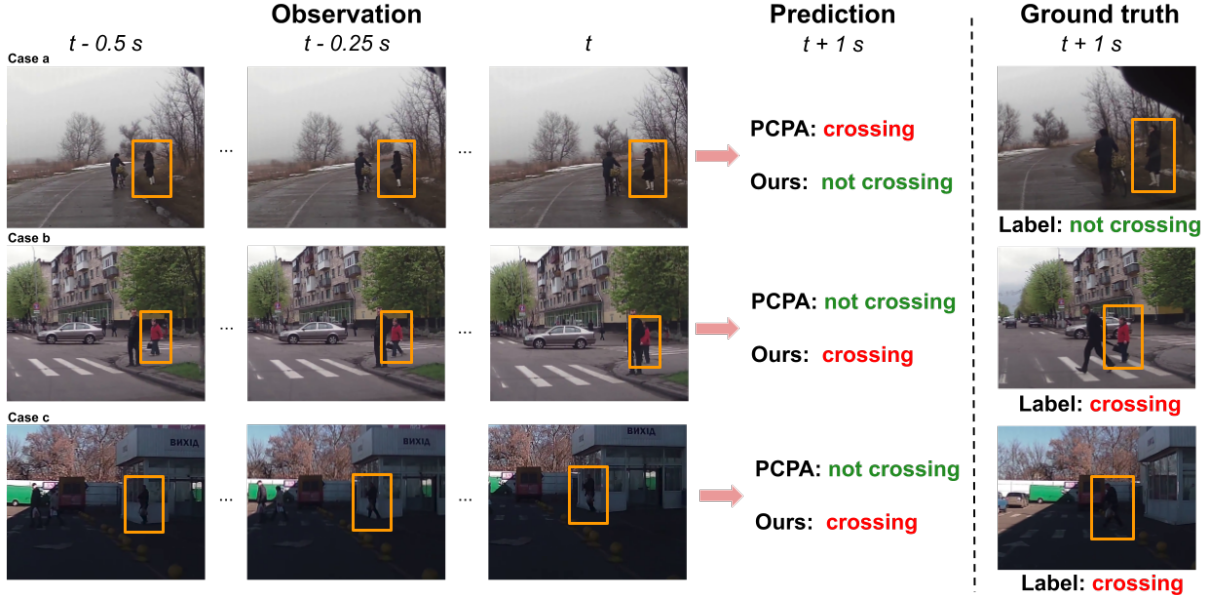


Fig. 3. Qualitative results on the JAAD dataset produced by PCPA [10] and our proposed model (Ours). The target pedestrians in images are enclosed as **bounding boxes**. The prediction results as well as ground truth labels are represented as **crossing** or **not crossing**.

frames are scaled to be the size of [224, 224] pixels, which is the same as the local context.

### C. Model architecture

The overall architecture is shown in Figure 2. It consists of CNN modules, RNN modules, attention modules, and a novel way of fusing different features.

**CNN module.** We use VGG19 [13] model pre-trained on ImageNet dataset [31] to build the CNN module. Sequential RGB images are collected as a 4D array input with the dimensions of [number of observed frames, row, cols, channels] ([16, 224, 224, 3] in this work), and then loaded by the CNN module. First, the feature map of every image from the fourth maxpooling layer of VGG19 is extracted with size [512, 14, 14]. Second, every feature map is averaged by a pooling layer with a  $14 \times 14$  kernel, and then flattened and concatenated, to obtain a final feature tensor with size [16, 512], as sequential visual features.

**RNN module.** We use gated recurrent unit (GRU) [16] to build the RNN module. The reason of choosing GRU is that GRU is more computationally efficient than its counterpart LSTM [15], which is older, and its architecture is relatively simple. The applied GRUs have 256 hidden units, which result in a feature tensor of size [16, 256].

**Attention module.** Attention module [32], by selectively focusing on parts of features, is used for better memorizing sequential sources. Sequential features (e.g. the output of RNN-based encoder) are represented as hidden states  $h = \{h_1, h_2, \dots, h_e\}$ . The attention weight is computed as:  $\alpha = \frac{\exp(score(h_e, h_s))}{\sum_{s'} \exp(score(h_e, h_{s'}))}$ , where  $score(h_e, h_s) = h_e^T W_s h_s$  and  $W_s$  is a weight matrix. Such attention weight trades off the end hidden state  $h_e$  with each previous source hidden state  $h_s$ . The output vector of the attention module is produced as

$V_{attention} = \tanh(W_c[h_e; h_s])$ , where  $W_c$  is a weight matrix, and  $h_c$  is the sum of all attention weighted hidden states as  $h_c = \sum_s \alpha h_s$ . The output of the attention module in our work is a feature tensor with size [1, 256].

**Hybrid fusion.** We applied a hybrid way of fusing the features from different sources. The strategy is shown in Figure 2. The proposed architecture has two branches, one for non-visual features and one for visual features.

The non-vision branch fuses three non-visual features (bounding boxes, pose keypoints, and vehicle speed). They are hierarchically fused according to their complexity and level of abstraction. The later stage of fusion, the closer impact of the fused feature on final prediction. This is illustrated in Figure 2(a). First, sequential pedestrian pose keypoints  $P_i$  are fed to a RNN-based encoder. Second, the output of the first stage is concatenated with 2D location trajectory  $L_i$  and fed to a new RNN-based encoder. Last, the output of the second stage is concatenated with ego-vehicle speed  $S$  and fed to a final RNN-based encoder. The output of the final encoder is then fed to an attention block to obtain the final non-visual feature vectors  $V_{nvi}$ .

The vision branch fuses two visual features, consisting of local context (enlarged pedestrian appearance around the bounding box) and global context (semantic segmentation of important objects in the whole scene), as shown in Figure 2(b). Local context  $C_{li}$  is encoded by first extracting spatial features from the CNN module (as explained in the previous section) and then extracting temporal features from the GRU module. Global context  $C_g$  is encoded in the same way. Both local and global features are then fed into their attention modules, and finally, concatenated together to generate final visual feature vectors  $V_{vi}$ .

Lastly, as shown in Figure 2(c), the final non-visual feature

TABLE I  
QUANTITATIVE RESULTS

Models	Model Variants			JAAD <sub>beh</sub>				JAAD <sub>all</sub>				Average		
	VE	GC	MFA	Acc	AUC	F1	P	R	Acc	AUC	F1	P	R	
SR [2]	VGG + GRU	<b>X</b>	<b>X</b>	0.59	0.52	0.71	0.64	0.80	0.79	0.76	0.54	0.44	0.71	0.65
SF-GRU [7]	VGG + GRU	<b>X</b>	hier.	0.58	<b>0.56</b>	0.65	<b>0.68</b>	0.62	0.76	0.77	0.53	0.40	0.79	0.63
PCPA [10]	3D CNN	<b>X</b>	later	0.53	0.53	0.59	0.66	0.53	0.76	0.79	0.55	0.41	<b>0.83</b>	0.62
Ours	VGG + GRU	<b>✓</b>	hybrid	<b>0.62</b>	0.54	<b>0.74</b>	0.65	<b>0.85</b>	<b>0.83</b>	<b>0.82</b>	<b>0.63</b>	<b>0.51</b>	0.81	<b>0.70</b>
<b>Ablations</b>														
Ours1	3D CNN	<b>✓</b>	later	0.59	0.53	0.69	0.65	0.75	0.77	0.77	0.54	0.42	0.76	0.65
Ours2	3D CNN	<b>✓</b>	early	0.59	0.54	0.69	0.65	0.74	0.77	0.74	0.51	0.41	0.69	0.63
Ours3	3D CNN	<b>✓</b>	hier.	0.57	0.48	0.70	0.62	0.81	0.78	0.77	0.55	0.43	0.75	0.65
Ours4	VGG + GRU	<b>X</b>	later	0.59	0.51	0.72	0.63	0.83	0.75	0.79	0.54	0.40	0.85	0.66
Ours5	VGG + GRU	<b>✓</b>	later	0.64	0.59	0.73	0.68	0.78	0.77	0.80	0.56	0.43	0.84	0.68
Ours6	VGG + GRU	<b>✓</b>	early	0.60	0.56	0.70	0.67	0.73	0.79	0.74	0.52	0.43	0.66	0.64
Ours7	VGG + GRU	<b>✓</b>	hier.	0.54	0.50	0.64	0.63	0.65	0.80	0.81	0.59	0.46	0.84	0.65

- The **bold** result means the best in the models.
- Acronyms: SR (SingleRNN), VE (Visual Encoder), GC (Global Context), MFA (Main Fusion Approach), Acc (Accuracy), AUC (Area under the ROC Curve), F1 (F1 score), P (Precision), R (Recall), early (early-fusion), later (later-fusion), hier. (hierarchical-fusion), hybrid (hybrid-fusion).

vectors  $V_{nvi}$  and the final visual feature vectors  $V_{vi}$  are concatenated and fed into another attention block, followed by a fully-connection (FC) layer to obtain the final predicted action  $A_i^{t+n} = f_{FC}(f_{attention}(V_{nvi}; V_{vi}))$ .

## IV. EXPERIMENTS

### A. Dataset and benchmark

We used JAAD dataset [1] for training and testing the proposed model. JAAD dataset provides two subsets, JAAD behavioral data (JAAD<sub>beh</sub>) and JAAD all data (JAAD<sub>all</sub>). JAAD<sub>beh</sub> contains pedestrians who are crossing (495) or are about to cross (191). JAAD<sub>all</sub> has additional pedestrians (2100) with non-crossing actions. We follow the same configuration of data preparation in [10], which uses a data sample overlap of 0.8, local context scale of 1.5. We adopt the evaluation metrics of accuracy, AUC, F1 score, precision and recall, as in the most updated benchmark of pedestrian action prediction [10].

### B. Implementation

We compared our proposed method with the following method: SingleRNN [2], SF-GRU [7] and PCPA[10]. For a fair comparison, all models were trained using the benchmark implementation released with PCPA model [10]. Other configuration follows the original PCPA module: dropout of 0.5 in the attention module, L2 regularization of 0.001 in FC layer, binary cross-entropy loss, Adam optimizer [33], learning rate =  $5 \times 10^{-7}$ , epochs = 40, and batch size = 2. All models were trained and tested on the same split of the dataset. Since JAAD dataset lacks ego-vehicle speed, the driver's actions provided by the dataset in the form of [stopped (0), moving slow (1), moving fast (2), decelerating (3), accelerating (4)] were used in place for the ego-vehicle speed in our experiments.

### C. Ablation study

An ablation study was also conducted to compare different strategies of fusing different features. In addition to baseline methods (SingRNN [2], SF-GRU [7] and PCPA [10]) and the proposed model (Ours), a total of 7 variants of the proposed model (Ours1, Ours2, ..., Ours7, as indicated in table I) were trained and compared with the proposed one. First, for the visual encoder, we tried (1) 2D CNN combined with RNN (VGG and GRU in our experiments) and (2) 3D CNN as proposed in the PCPA model. Second, we tried the models with and without the global feature (semantic segmentation). Last, we tried different fusion strategies that include later fusion, early fusion, and hierarchical fusion so that they can be compared with the proposed hybrid fusion strategy. Later fusion is the same as the one proposed in PCPA [10]. Early fusion concatenates non-visual features and visual features directly and then send them into one RNN module followed by an attention module. Hierarchical fusion gradually fused both visual features and non-visual features by RNN modules using the similar way in Figure 2(a), and then an attention module is applied.

## V. RESULTS

**Quantitative Results.** The comprehensive and quantitative results are shown table I, which reports the accuracy, AUC, F1 score, precision, and recall. Compared to the baseline models of SingleRNN [2], SF-GRU [7] and PCPA [10], our proposed model achieved the best performance on average, and the best scores of accuracy, F1, and recall in JAAD<sub>beh</sub> and accuracy, AUC, F1, precision in JAAD<sub>all</sub>. The average score of the proposed outperforms the best baseline with at least 5% improvement. The ablation results show that even only introducing global context can improve the accuracy. This is confirmed by comparing Ours1 with PCPA model and Ours5 with Ours4. Using 2D CNN plus RNN instead of 3D CNN for visual feature encoding also has the advantage of extracting spatio-temporal features. This is

demonstrated by comparing Ours4 with PCPA. In terms of fusion strategies, the proposed hybrid fusion achieved the best performance, which can be identified by comparing Ours with Ours5, Ours6, and Ours7.

**Qualitative Results.** Figure 3 shows some qualitative examples of pedestrian crossing intention prediction. We mainly compare the proposed method with PCPA model. In the provided examples, our method correctly predicted the intention of pedestrian crossing but the PCPA failed. Taking a closer look at the examples, the following argument is raised. Without utilizing the global context, the task of crossing intention prediction may face the problems of (1) unknown direction of the pedestrian (Case a in Figure 3), (2) occlusion (Case b in Figure 3), and (3) poor vision (Case c in Figure 3). Global context can provide additional information to account for the interaction between the whole scene and the target pedestrian.

## VI. CONCLUSIONS

In this work, we proposed a novel method for vision-based pedestrian crossing intention prediction. Our method explicitly considers the global context as a channel representing the interaction between the target pedestrian and the whole scene. We also proposed a hybrid fusion strategy for different features using 2D CNNs, RNNs, and attention mechanisms. Experiments on the JAAD dataset show that the proposed method achieves the state-of-the-art against baseline methods in the pedestrian action prediction benchmark.

Future work can focus on improving our model’s robustness in unexpected situations, e.g., poor vision and occlusion. Additionally, feature fusion with more information sources can be explored. Finally, fine-tuning the model for particular pedestrian subsets, such as children and disabled people, can increase overall safety and performance.

## ACKNOWLEDGMENT

Material reported here was supported by the United States Department of Transportation under Award Number 69A3551747111 for the Mobility21 University Transportation Center.

## REFERENCES

- [1] A. Rasouli, I. Kotseruba, and J. K. Tsotsos, “Are they going to cross? a benchmark dataset and baseline for pedestrian crosswalk behavior,” in *Proceedings of the IEEE International Conference on Computer Vision Workshops*, 2017, pp. 206–213.
- [2] I. Kotseruba, A. Rasouli, and J. K. Tsotsos, “Do they want to cross? understanding pedestrian intention for behavior prediction,” in *2020 IEEE Intelligent Vehicles Symposium (IV)*. IEEE, 2020, pp. 1688–1693.
- [3] J. Lorenzo, I. Parra, F. Wirth, C. Stiller, D. F. Llorca, and M. A. Sotelo, “Rnn-based pedestrian crossing prediction using activity and pose-related features,” in *2020 IEEE Intelligent Vehicles Symposium (IV)*. IEEE, 2020, pp. 1801–1806.
- [4] A. Rasouli, I. Kotseruba, T. Kunic, and J. K. Tsotsos, “Pie: A large-scale dataset and models for pedestrian intention estimation and trajectory prediction,” in *Proceedings of the IEEE/CVF International Conference on Computer Vision*, 2019, pp. 6262–6271.
- [5] Z. Fang and A. M. López, “Is the pedestrian going to cross? answering by 2d pose estimation,” in *2018 IEEE Intelligent Vehicles Symposium (IV)*. IEEE, 2018, pp. 1271–1276.
- [6] F. Piccoli, R. Balakrishnan, M. J. Perez, M. Sachdeo, C. Nunez, M. Tang, K. Andreasson, K. Bjurek, R. D. Raj, E. Davidsson, *et al.*, “Fussi-net: Fusion of spatio-temporal skeletons for intention prediction network,” *arXiv preprint arXiv:2005.07796*, 2020.
- [7] A. Rasouli, I. Kotseruba, and J. K. Tsotsos, “Pedestrian action anticipation using contextual feature fusion in stacked rnns,” in *BMVC*, 2019.
- [8] A. Rasouli, T. Yau, M. Rohani, and J. Luo, “Multi-modal hybrid architecture for pedestrian action prediction,” *arXiv preprint arXiv:2012.00514*, 2020.
- [9] A. Rasouli, M. Rohani, and J. Luo, “Pedestrian behavior prediction via multitask learning and categorical interaction modeling,” *arXiv preprint arXiv:2012.03298*, 2020.
- [10] I. Kotseruba, A. Rasouli, and J. K. Tsotsos, “Benchmark for evaluating pedestrian action prediction,” in *Proceedings of the IEEE/CVF Winter Conference on Applications of Computer Vision*, 2021, pp. 1258–1268.
- [11] J. Hariyono and K.-H. Jo, “Detection of pedestrian crossing road,” in *2015 IEEE International Conference on Image Processing (ICIP)*. IEEE, 2015, pp. 4585–4588.
- [12] P. Dollár, C. Wojek, B. Schiele, and P. Perona, “Pedestrian detection: A benchmark,” in *2009 IEEE Conference on Computer Vision and Pattern Recognition*. IEEE, 2009, pp. 304–311.
- [13] K. Simonyan and A. Zisserman, “Very deep convolutional networks for large-scale image recognition,” in *3rd International Conference on Learning Representations, ICLR 2015, San Diego, CA, USA, May 7-9, 2015, Conference Track Proceedings*, Y. Bengio and Y. LeCun, Eds., 2015. [Online]. Available: <http://arxiv.org/abs/1409.1556>
- [14] B. Liu, E. Adeli, Z. Cao, K.-H. Lee, A. Shenoi, A. Gaidon, and J. C. Niebles, “Spatiotemporal relationship reasoning for pedestrian intent prediction,” *IEEE Robotics and Automation Letters*, vol. 5, no. 2, pp. 3485–3492, 2020.
- [15] S. Hochreiter and J. Schmidhuber, “Long short-term memory,” *Neural computation*, vol. 9, no. 8, pp. 1735–1780, 1997.
- [16] K. Cho, B. van Merriënboer, D. Bahdanau, and Y. Bengio, “On the properties of neural machine translation: Encoder–decoder approaches,” *Syntax, Semantics and Structure in Statistical Translation*, p. 103, 2014.
- [17] D. Tran, L. Bourdev, R. Fergus, L. Torresani, and M. Paluri, “Learning spatiotemporal features with 3d convolutional networks,” in *Proceedings of the IEEE international conference on computer vision*, 2015, pp. 4489–4497.
- [18] K. Saleh, M. Hossny, and S. Nahavandi, “Real-time intent prediction of pedestrians for autonomous ground vehicles via spatio-temporal densenet,” in *2019 International Conference on Robotics and Automation (ICRA)*. IEEE, 2019, pp. 9704–9710.
- [19] ———, “Spatio-temporal densenet for real-time intent prediction of pedestrians in urban traffic environments,” *Neurocomputing*, vol. 386, pp. 317–324, 2020.
- [20] M. Chaabane, A. Trabelsi, N. Blanchard, and R. Beveridge, “Looking ahead: Anticipating pedestrians crossing with future frames prediction,” in *Proceedings of the IEEE/CVF Winter Conference on Applications of Computer Vision*, 2020, pp. 2297–2306.
- [21] P. Gujjar and R. Vaughan, “Classifying pedestrian actions in advance using predicted video of urban driving scenes,” in *2019 International Conference on Robotics and Automation (ICRA)*. IEEE, 2019, pp. 2097–2103.
- [22] Z. Fang and A. M. López, “Intention recognition of pedestrians and cyclists by 2d pose estimation,” *IEEE Transactions on Intelligent Transportation Systems*, vol. 21, no. 11, pp. 4773–4783, 2019.
- [23] Z. Wang and N. Papanikolopoulos, “Estimating pedestrian crossing states based on single 2d body pose,” in *Proceedings of the IEEE International Conference on Intelligent Robots and Systems (IROS)*, vol. 2, 2020.
- [24] P. R. G. Cadena, M. Yang, Y. Qian, and C. Wang, “Pedestrian graph: Pedestrian crossing prediction based on 2d pose estimation and graph convolutional networks,” in *2019 IEEE Intelligent Transportation Systems Conference (ITSC)*. IEEE, 2019, pp. 2000–2005.
- [25] A. Rasouli, T. Yau, P. Lakner, S. Malekmohammadi, M. Rohani, and J. Luo, “Pepsscenes: A novel dataset and baseline for pedestrian action prediction in 3d,” *arXiv preprint arXiv:2012.07773*, 2020.
- [26] J. Redmon and A. Farhadi, “Yolov3: An incremental improvement,” *arXiv preprint arXiv:1804.02767*, 2018.
- [27] N. Wojke, A. Bewley, and D. Paulus, “Simple online and realtime tracking with a deep association metric,” in *2017 IEEE international conference on image processing (ICIP)*. IEEE, 2017, pp. 3645–3649.

- [28] Z. Cao, G. Hidalgo, T. Simon, S.-E. Wei, and Y. Sheikh, “Openpose: realtime multi-person 2d pose estimation using part affinity fields,” *IEEE transactions on pattern analysis and machine intelligence*, vol. 43, no. 1, pp. 172–186, 2019.
- [29] L.-C. Chen, G. Papandreou, F. Schroff, and H. Adam, “Rethinking atrous convolution for semantic image segmentation,” *arXiv preprint arXiv:1706.05587*, 2017.
- [30] M. Cordts, M. Omran, S. Ramos, T. Rehfeld, M. Enzweiler, R. Benenson, U. Franke, S. Roth, and B. Schiele, “The cityscapes dataset for semantic urban scene understanding,” in *Proceedings of the IEEE conference on computer vision and pattern recognition*, 2016, pp. 3213–3223.
- [31] J. Deng, W. Dong, R. Socher, L.-J. Li, K. Li, and L. Fei-Fei, “Imagenet: A large-scale hierarchical image database,” in *2009 IEEE conference on computer vision and pattern recognition*. Ieee, 2009, pp. 248–255.
- [32] M.-T. Luong, H. Pham, and C. D. Manning, “Effective approaches to attention-based neural machine translation,” in *Proceedings of the 2015 Conference on Empirical Methods in Natural Language Processing*, 2015, pp. 1412–1421.
- [33] D. P. Kingma and J. Ba, “Adam: A method for stochastic optimization,” *arXiv preprint arXiv:1412.6980*, 2014.